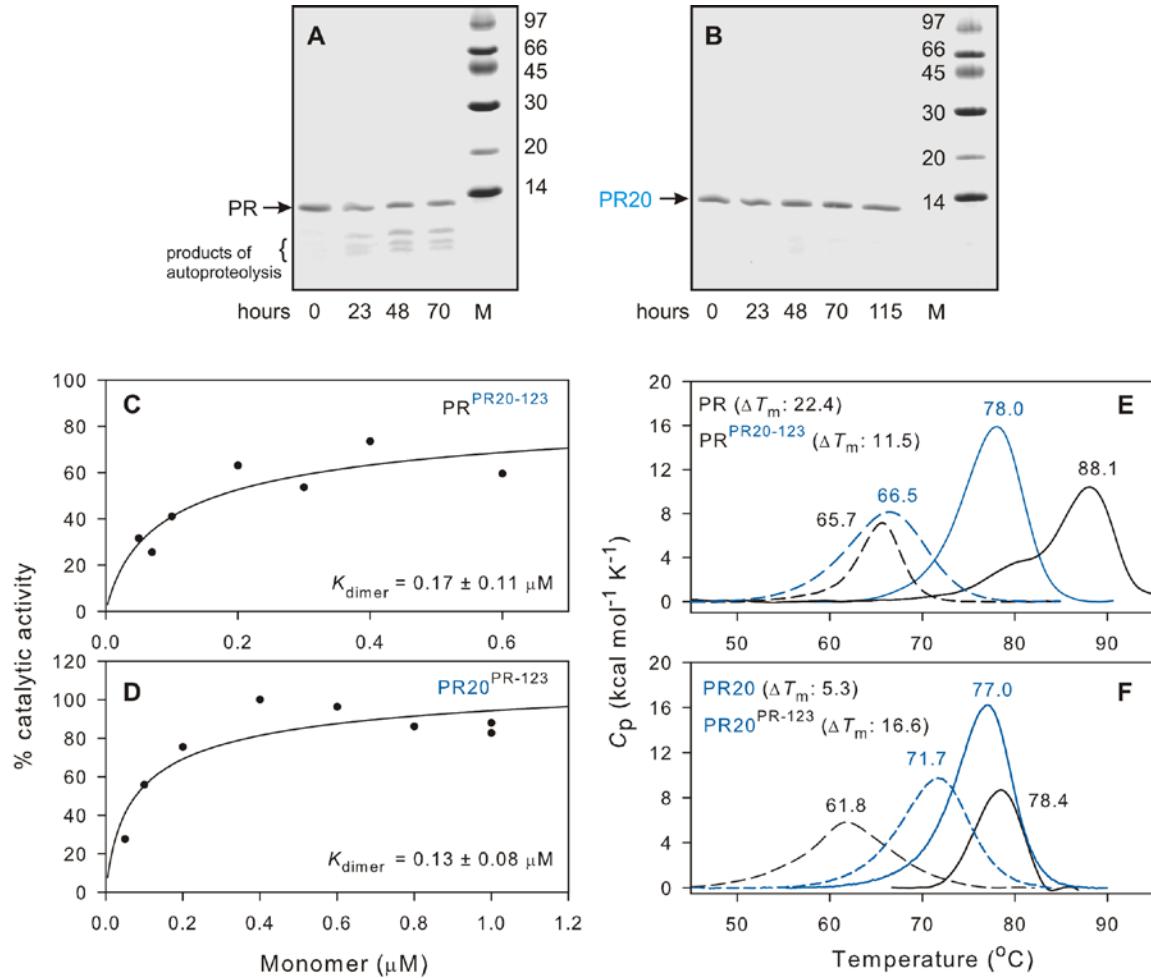


**Supporting Information:**

**Mutations Proximal to Sites of Autoproteolysis and the  $\alpha$ -Helix that Co-evolve  
under Drug Pressure Modulate the Autoprocessing and Vitality of HIV-1  
Protease**

John M. Louis\*, Lalit Deshmukh, Jane M. Sayer, Annie Aniana and G. Marius Clore

**Figure S1**

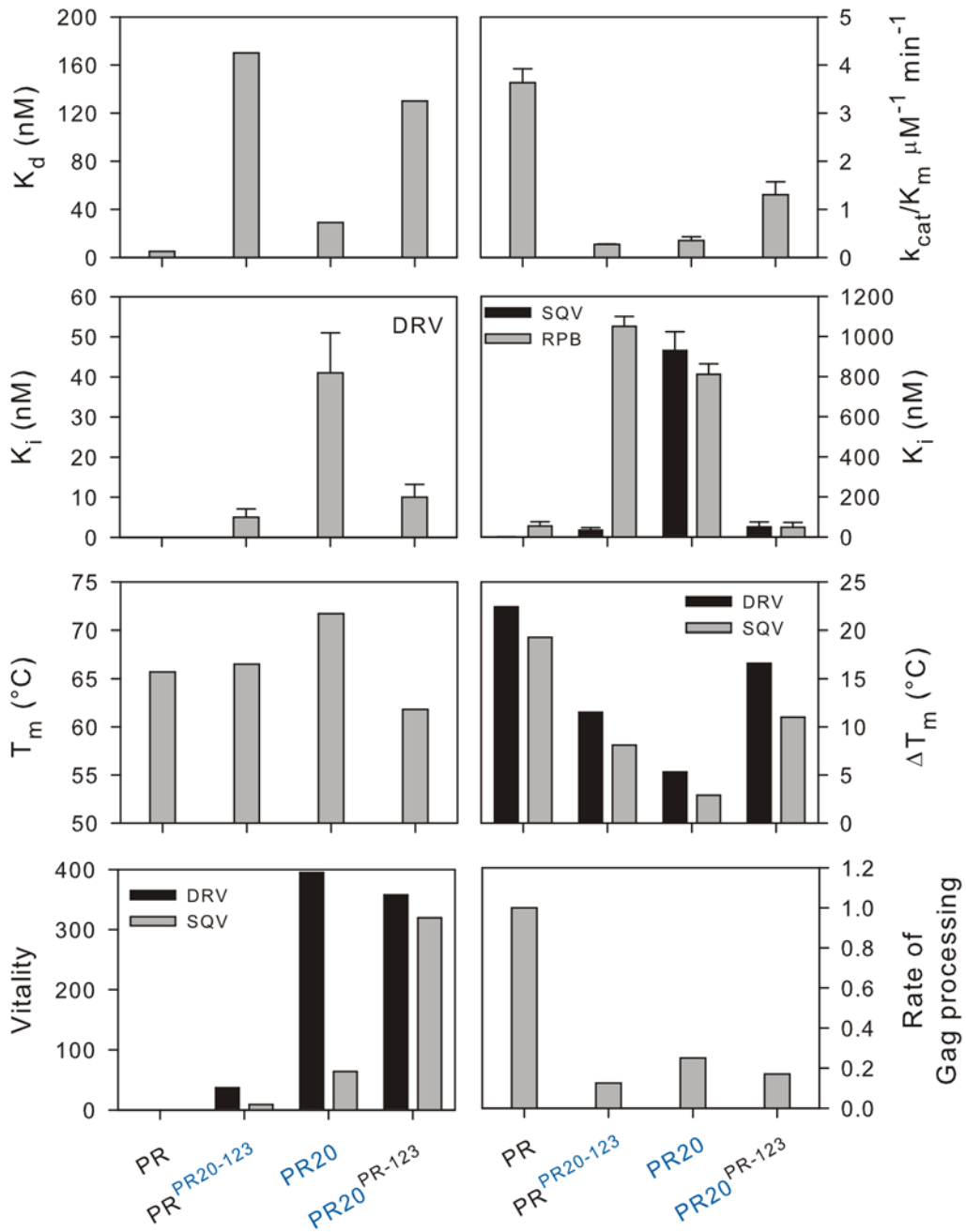


**Figure S1.** Evaluation of the autoproteolysis,  $K_{\text{dimer}}$  and thermal melting of mature proteases. Published results of the time course of autoproteolysis of PR (A) and PR20 (B) by SDS-PAGE are shown here solely for comparison with PR<sup>PR20-123</sup> and PR20<sup>PR-123</sup> described in the main text.<sup>1</sup>  $K_{\text{dimer}}$  of PR<sup>PR20-123</sup> (B) and PR20<sup>PR-123</sup> (C) in 50 mM sodium acetate, pH 5.0, containing 250 mM sodium chloride at 28  $^{\circ}\text{C}$ .  $K_{\text{dimer}}$  values were determined by fitting a previously described equation<sup>2</sup> (shown below) to rate data, where  $\text{PR}_{\text{mono}}$  is the concentration of PR expressed as monomers,  $V_x$  is the observed initial rate/ $[\text{PR}_{\text{mono}}]$ , and  $V_{\text{max}}$  is the extrapolated maximum rate/ $[\text{PR}_{\text{mono}}]$  when the enzyme is fully dimeric. Data shown are scaled relative to a maximum activity of 100%.

$$V_x = V_{\text{max}} \left[ 1 - \left\{ (K_{\text{dimer}}/2 * [\text{PR}_{\text{mono}}])^{1/2} * [(K_{\text{dimer}}/2 * [\text{PR}_{\text{mono}}]) + 4]^{1/2} - (K_{\text{dimer}}/2 * [\text{PR}_{\text{mono}}])^{1/2} \right\} / 2 \right]$$

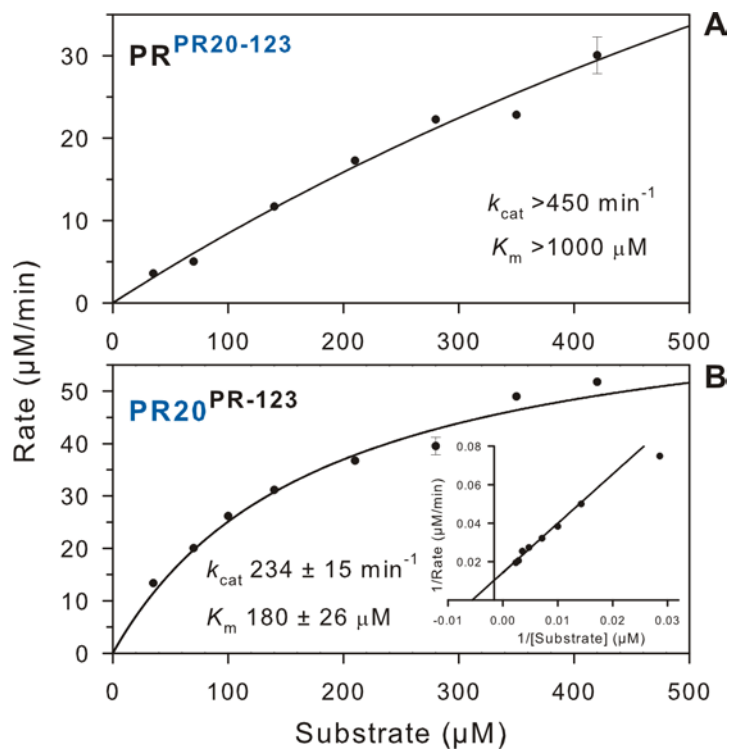
DSC thermograms of PR<sup>PR20-123</sup> (E) PR20<sup>PR-123</sup> (F) and their parent constructs PR and PR20, in the presence (solid lines) and absence (dashed lines) of a two-fold molar excess of darunavir. Data from previous work are shown for PR<sup>3</sup> and PR20<sup>1</sup> for comparison only.

**Figure S2**



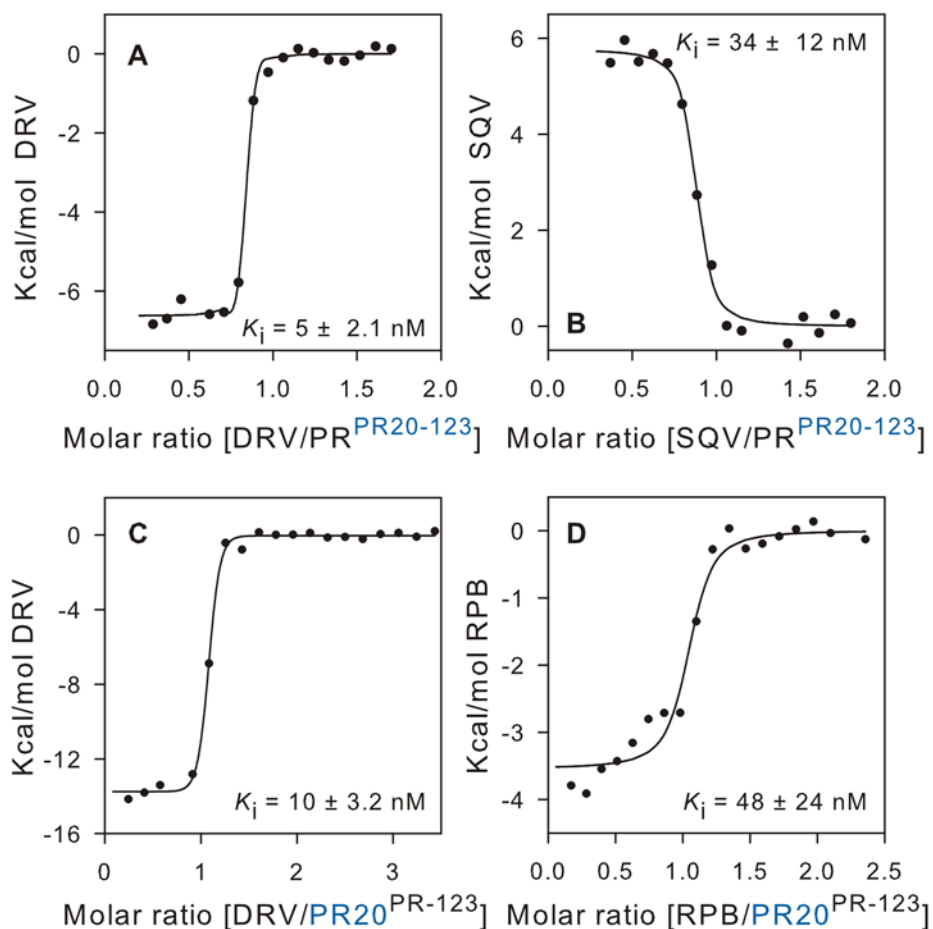
**Figure S2.** Graphical representation of table 1.

Figure S3



**Figure S3.** Michaelis-Menten plots for hydrolysis of chromogenic substrate (measured at 310 nm) by  $0.3 \mu\text{M}$  PR<sup>PR20-123</sup> (A) and PR20<sup>PR-123</sup> (B) in 50 mM sodium acetate, pH 5.0, containing 250 mM sodium chloride at 28 °C. As higher substrate concentrations ( $> 450 \mu\text{M}$ ) lead to weak inhibition by one of the cleavage products, the highest substrate concentration that could be used is below  $K_m$  for PR<sup>PR20-123</sup> (A). Thus, only the estimated lower limits for these kinetic parameters are given. For PR20<sup>PR-123</sup> (B) both Michaelis-Menten and Lineweaver-Burk plots are shown.

**Figure S4**



**Figure S4.** Determination of  $K_i$  ( $1/K_{\text{association}}$ ) for binding of inhibitors to PR<sup>20-123</sup> and PR20<sup>PR-123</sup> by ITC in 50 mM sodium acetate, pH 5.0, at 28 °C. For competitive inhibitors,  $1/K_{\text{association}}$  for inhibitor binding by ITC is the same as determined kinetically.<sup>4</sup> The apparent stoichiometry (N-value, indicated by the midpoint of the binding isotherm) for both titrations of PR20<sup>PR-123</sup>, was lower than expected for the 1:1 ratio of the enzyme-inhibitor complex, likely due to autoproteolysis (see Figure 2). Therefore, the concentration was scaled in panels (C) and (D) to give an N-value of 1. No concentration correction was applied for PR<sup>20-123</sup> [panels (A) and (B)] as expected. DRV, SQV and RPB denote darunavir, saquinavir and reduced peptide bond inhibitor, respectively.

**Figure S5**

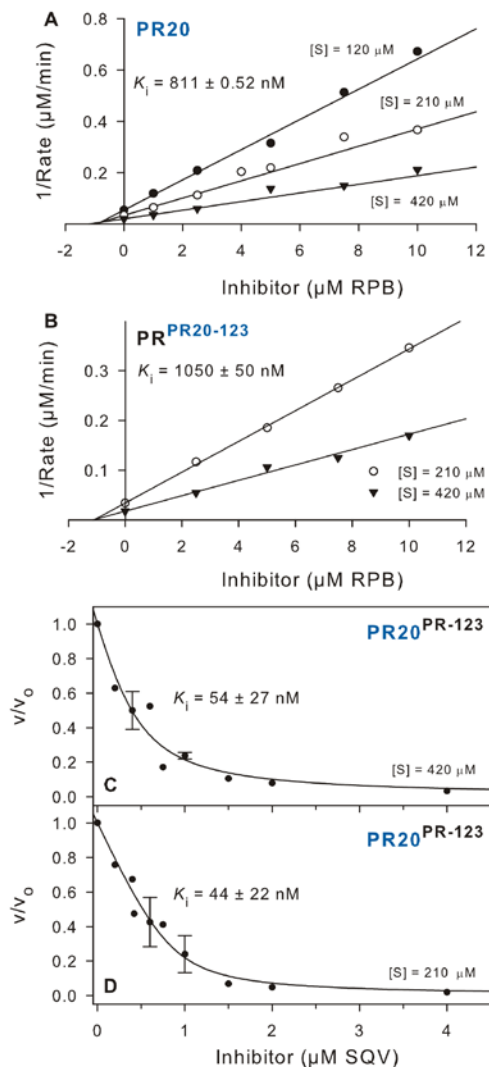


**Figure S5.**  $K_i$  determination for reduced peptide bond inhibitor (RPB) binding to (A) 0.5  $\mu\text{M}$  PR20 and (B) 0.6  $\mu\text{M}$  PR<sup>PR20-123</sup> by use of Dixon plots for hydrolysis of chromogenic substrate. Each complete data set comprising 2 or 3 substrate concentrations was processed together by use of the enzyme kinetics module of Sigmaplot 10. (C and D) Kinetic determinations of  $\text{IC}_{50}$  and  $K_i$  for saquinavir (SQV) mediated inhibition of 0.54  $\mu\text{M}$  PR<sup>PR-123</sup> at two substrate concentrations. For duplicate measurements average values with error bars are shown. The solid lines are curve fits of the Morrison equation<sup>5</sup> (shown below) to the data with parameters  $\text{IC}_{50}$  and  $E$ , where  $V_o$  and  $V_{\text{obs}}$  are initial rates in the absence and presence of inhibitor, respectively, and  $I$  and  $E$  are total concentrations of inhibitor and active sites respectively.

$$V_{\text{obs}}/V_o = 1 - \left\{ \left[ I + E + \text{IC}_{50} - \left[ (I + E + \text{IC}_{50})^2 - 4 * I * E \right]^{1/2} \right] / 2 * E \right\}$$

$K_i$  values shown were calculated from  $\text{IC}_{50}$  by use of the equation  $K_i = \text{IC}_{50} / (1 + [\text{Substrate}] / K_m)$ .

**Figure S6**

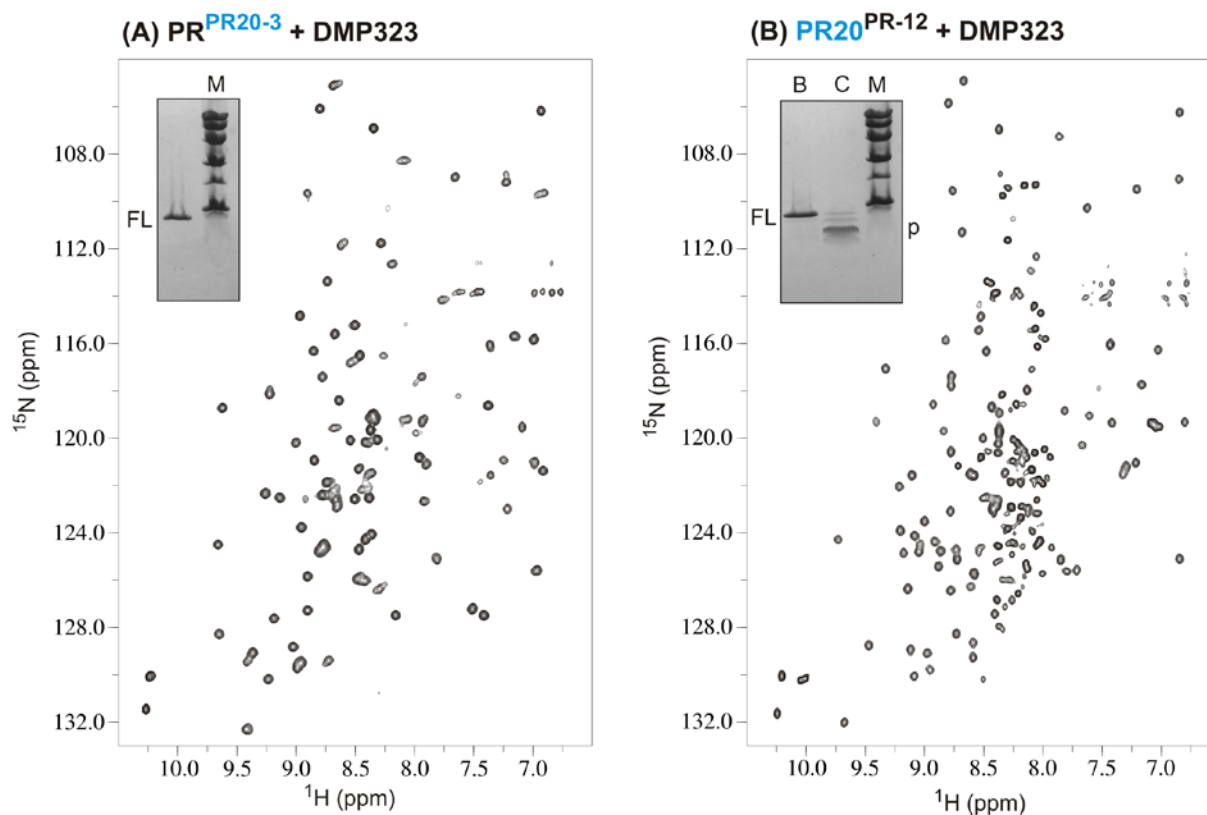


**Figure S6.** 600 MHz  $^1\text{H}$ - $^{15}\text{N}$  TROSY correlation spectra of freshly prepared  $^{15}\text{N}$  or  $^{15}\text{N}/^{13}\text{C}$  labeled proteins in 20 mM sodium phosphate buffer, pH 5.7, 20 °C. Spectra were acquired in the presence of the symmetric inhibitor DMP323.<sup>6</sup> After acquiring the NMR spectra, samples were subjected to SDS-PAGE on homogeneous 20% Phastgels and stained with Phastgel blue R to visualize the bands. Inset lanes B and C denote PR<sup>PR-12</sup> + DMP323 and PR<sup>PR-12</sup>, respectively. PR<sup>PR-12</sup> undergoes rapid autoproteolysis in the absence of DMP323. M, FL and p denote molecular weight standards in kDa, full-length mature protease and products of autoproteolysis, respectively.

## REFERENCES

1. Louis, J. M., Tozser, J., Roche, J., Matuz, K., Aniana, A., and Sayer, J. M. (2013) Enhanced stability of monomer fold correlates with extreme drug resistance of HIV-1 protease. *Biochemistry* 52, 7678-7688.
2. Sayer, J. M., Agniswamy, J., Weber, I. T., and Louis, J. M. (2010) Autocatalytic maturation, physical/chemical properties, and crystal structure of group N HIV-1 protease: relevance to drug resistance. *Protein Sci.* 19, 2055-2072.
3. Sayer, J. M., Liu, F., Ishima, R., Weber, I. T., and Louis, J. M. (2008) Effect of the active site D25N mutation on the structure, stability, and ligand binding of the mature HIV-1 protease. *J. Biol. Chem.* 283, 13459-13470.
4. Brower, E. T., Bacha, U. M., Kawasaki, Y., and Freire, E. (2008) Inhibition of HIV-2 protease by HIV-1 protease inhibitors in clinical use. *Chem. Biol. Drug Des* 71, 298-305.
5. Furfine, E. S. (2000) Identifying and Characterizing HIV Protease Inhibitors. *Methods Mol. Med.* 24, 313-325.
6. Lam, P. Y., Ru, Y., Jadhav, P. K., Aldrich, P. E., DeLucca, G. V., Eyermann, C. J., Chang, C. H., Emmett, G., Holler, E. R., Daneker, W. F., Li, L., Confalone, P. N., McHugh, R. J., Han, Q., Li, R., Markwalder, J. A., Seitz, S. P., Sharpe, T. R., Bacheler, L. T., Rayner, M. M., Klabe, R. M., Shum, L., Winslow, D. L., Kornhauser, D. M., Hodge, C. N., and . (1996) Cyclic HIV protease inhibitors: synthesis, conformational analysis, P2/P2' structure-activity relationship, and molecular recognition of cyclic ureas. *J. Med. Chem.* 39, 3514-3525.